Author Manuscript

Author Manuscript

Author Manuscript

Author Manuscript

HHS Public Access

Author manuscript

Curr Biol. Author manuscript; available in PMC 2020 May 05.

Published in final edited form as:

Curr Biol. 2019 October 21; 29(20): 3359–3369.e4. doi:10.1016/j.cub.2019.08.003.

Neuronal O-GlcNAcylation Improves Cognitive Function in the Aged Mouse Brain

Elizabeth G. Wheatley[1,2], **Eddy Albarran**[3,4], **Charles W. White III**[1,2], **Gregor Bieri**[1], **Cesar Sanchez-Diaz**[1], **Karishma Pratt**[1,2], **Cedric E. Snethlage**[1], **Jun B. Ding**[3,4], **Saul A. Villeda**[1,2,5,6,7,*]

[1]Department of Anatomy, University of California, San Francisco, San Francisco, CA 94143, USA

[2]Developmental and Stem Cell Biology Graduate Program, University of California, San Francisco, San Francisco, CA 94143, USA

[3]Neuroscience IDP Program, Stanford University School of Medicine, Stanford, CA 94305, USA

[4]Department of Neurosurgery, Stanford University School of Medicine, Palo Alto, CA 94304, USA

[5]Department of Physical Therapy and Rehabilitation Science, University of California, San Francisco, San Francisco, CA 94143, USA

[6]The Eli and Edythe Broad Center for Regeneration Medicine and Stem Cell Research, San Francisco, CA 94143, USA

[7]Lead Contact

SUMMARY

Mounting evidence in animal models indicates potential for rejuvenation of cellular and cognitive functions in the aging brain. However, the ability to utilize this potential is predicated on identifying molecular targets that reverse the effects of aging in vulnerable regions of the brain, such as the hippocampus. The dynamic post-translational modification O-linked N-Acetylglucosamine (O-GlcNAc) has emerged as an attractive target for regulating aging-specific synaptic alterations as well as neurodegeneration. While speculation exists about the role of O-GlcNAc in neurodegenerative conditions, such as Alzheimer's disease, its role in physiological brain aging remains largely unexplored. Here, we report that countering age-related decreased O-GlcNAc transferase (OGT) expression and O-GlcNAcylation ameliorates cognitive impairments in aged mice. Mimicking an aged condition in young adults by abrogating OGT, using a temporally

This is an open access article under the CC BY-NC-ND license (http://creativecommons.org/licenses/by-nc-nd/4.0/).

*Correspondence: saul.villeda@ucsf.edu.

AUTHOR CONTRIBUTIONS

E.G.W. and S.A.V. developed concept and designed experiments. E.G.W. collected and analyzed data. E.G.W. and C.W.W. performed histological and biochemical studies. E.A. and J.B.D. performed electrophysiological studies. E.G.W., C.S.-D., K.P., and C.E.S. performed cognitive studies. E.G.W., G.B., and C.W.W generated and validated viral constructs. E.G.W. and G.B generated schematics. E.G.W and S.A.V wrote the manuscript. S.A.V supervised all aspects of this project. All authors had the opportunity to discuss results and comment on manuscript.

SUPPLEMENTAL INFORMATION

Supplemental Information can be found online at https://doi.Org/10.1016/j.cub.2019.08.003.

DECLARATION OF INTERESTS

The authors declare no competing interests.

Author Manuscript Author Manuscript Author Manuscript Author Manuscript

controlled neuron-specific conditional knockout mouse model, recapitulated cellular and cognitive features of brain aging. Conversely, overexpressing OGT in mature hippocampal neurons using a viral-mediated approach enhanced associative fear memory in young adult mice. Excitingly, in aged mice overexpressing neuronal OGT in the aged hippocampus rescued in part age-related impairments in spatial learning and memory as well as associative fear memory. Our data identify O-GlcNAcylaton as a key molecular mediator promoting cognitive rejuvenation.

Graphical Abstract

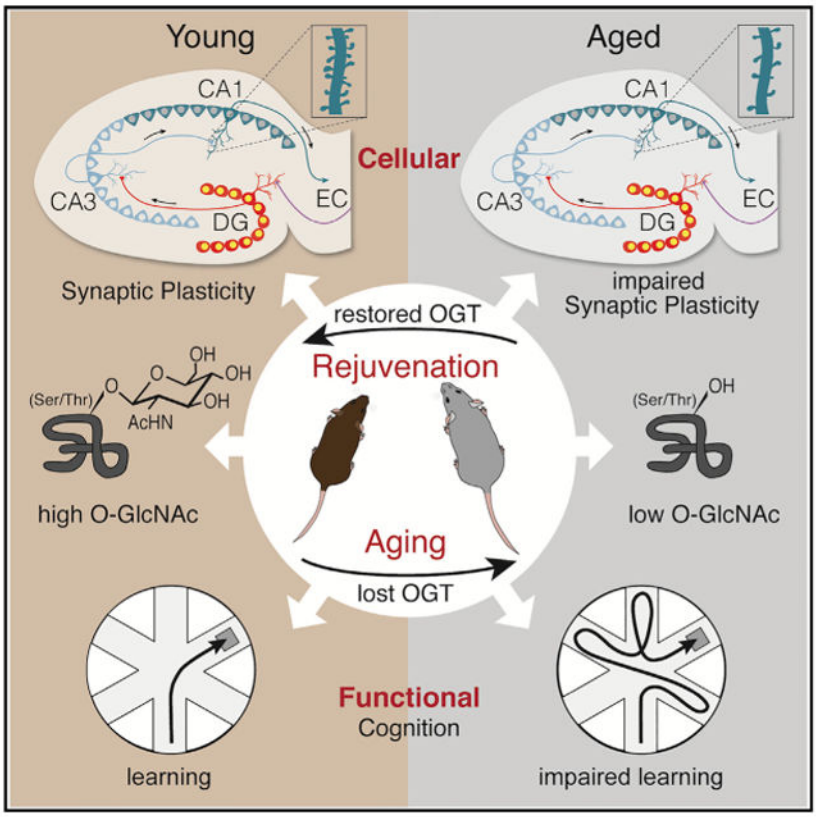

In Brief

Wheatley et al. identify O-GlcNAcylation as a key posttranslational modification promoting cognitive rejuvenation. Mimicking age-related decreased neuronal OGT and O-GlcNAc levels in the young hippocampus impaired cognition, while restoring neuronal OGT and O-GlcNAc in the aged hippocampus rejuvenated cognition.

INTRODUCTION

It has become clear that cognitive dysfunction in the aged brain is not paralleled by gross neurodegeneration but by synaptic and plasticity-related molecular alterations [1-5], impairments of which are believed to facilitate later onset of dementia-related neurodegenerative diseases. It is therefore critical to gain mechanistic insight into the molecular mediators that drive aging in the brain and consequently underlie age-related

Author Manuscript Author Manuscript Author Manuscript Author Manuscript

vulnerability to neurodegenerative diseases. Indeed, identifying such molecular mediators may provide potential targets by which to rejuvenate the aged brain and counteract the effects of aging that promote the onset of neurodegenerative diseases, such as Alzheimer's disease.

Recent work proposes the dynamic form of intracellular protein glycosylation, O-linked N-Acetylglucosamine (O-GlcNAc), as an attractive target for regulating aging-specific synaptic and plasticity-related molecular alterations, as well as neurodegenerative phenotypes [6-11]. O-GlcNAcylation is regulated by two enzymes–O-GlcNAc transferase (OGT) and O-GlcNAcase (OGA)–which catalyze the addition and removal of O-GlcNAc to serine and threonine residues of proteins, respectively. To date, this dynamic post-translational modification has been shown to mediate various aspects of synaptic plasticity underlying learning and memory formation in the adult mouse hippocampus [12-19]. Analyses of synaptic terminal preparations isolated from brain tissue in young mice have identified high O-GlcNAcylation on synaptic proteins [6-9]. Acute pharmacological manipulations of global O-GlcNAc mediate both long-term potentiation (LTP) and long-term depression (LTD) in hippocampal slices; two critical physiological synaptic processes regulating memory formation [13, 18]. Furthermore, reducing levels of O-GlcNAcylation *in vitro* decreases dendritic spine density in primary neurons [19]. Interestingly, constitutive loss of Ogt in *C. elegans* elicits neurodegenerative phenotypes and results in shortened lifespan [20, 21]. Similarly, in genetic knockout mouse models, embryonic loss of neuronal OGT elicits early death in postnatal mice [22], while constitutive loss in forebrain neurons elicits neurodegeneration in adult mice [8]. There is much speculation about the role of O-GlcNAc within the context of neurodegenerative conditions. However, while O-GlcNAc levels decrease in the adult brain during both normal aging [23] and Alzheimer's disease [6, 8, 24], the role of O-GlcNAcylation in contributing to physiological brain aging has been largely overlooked.

In this study, we report that countering age-related decreased O-GlcNAcylation rescues cognitive impairments in the aged mouse hippocampus. We detect decreased OGT expression and lower O-GlcNAc levels in the aged hippocampus, concomitant with age-related synaptic and cognitive impairments. Mimicking an age-related loss of O-GlcNAcylation by targeting OGT in adult neurons reduces expression of plasticity-related markers and dendritic spine density in the hippocampus of adult mice. Moreover, acute loss of neuronal O-GlcNAcylation impairs hippocampal-dependent learning and memory processes. Excitingly, increasing neuronal O-GlcNAcylation by overexpressing OGT in the hippocampus enhances associative fear memory in young animals, while improving spatial learning and memory, as well as associative fear memory in aged mice. Our findings posit decreased O-GlcNAcylation as a driver of synaptic and cognitive decline in the aging brain, with functional implications for cognitive rejuvenation.

Author Manuscript Author Manuscript Author Manuscript Author Manuscript

RESULTS

Decreased OGT Expression and O-GlcNAcylation Accompany Neuronal and Cognitive Hallmarks of Brain Aging in the Hippocampus

The hippocampus (comprising the CA1, CA3, and dentate gyrus [DG] sub-regions) is a particularly vulnerable brain region to the effects of aging, exhibiting stereotypical hallmarks that include downregulation of plasticity-related genes, reduced dendritic spine density, decreased synaptic plasticity, and impairments in associated cognitive functions [25]. Therefore, to begin our investigation, we assessed how OGT expression and O-GlcNAcylation broadly change with age in the adult hippocampus. We profiled hippocampal lysates from young and aged wild-type mice and observed a decrease in OGT protein levels, as well as a decrease in global protein O-GlcNAcylation with age (Figures 1A and 1B).

Next, we established a reference point for characteristic hallmarks of hippocampal aging reported to be amenable to brain rejuvenation [26-29]. First, we assessed the levels of the activated phosphorylated form of the transcription factor CREB (pCREB)–previously demonstrated to underlie improvements in hippocampal-dependent cognitive function in the aged brain [26, 29], and whose O-GlcNAcylation status regulates amygdala-dependent memory formation [16]. We detected an age-dependent decrease in pCREB (Figures 1C and 1D) concomitant with decreased expression of cFos (Figures 1C and 1E), an immediate early gene downstream of CREB also implicated in cognitive rejuvenation [28]. No widespread cell loss or neurodegenerative phenotypes were observed by Nissl body staining (Figures 1C and 1F) or DAPI-mediated cell counts (Figure S1A). To profile synaptic structural changes in hippocampal neurons, we employed Golgi staining and observed an age-dependent decrease in tertiary dendritic spine density in CA1 pyramidal and DG granular neurons (Figure 1G). Additionally, we examined the expression of several synaptic markers in hippocampal lysates from young or aged mice by western blot analysis. We observed an age-dependent decrease in subunits 2A and 2B of the post-synaptic Glutamate NMDA receptor (NR2A; NR2B) and a corresponding increase in the NR2A/NR2B ratio (Figures 1H and 1I), often used as an indicator for synaptic function [30]. No changes were detected for the post-synaptic scaffolding protein PSD-95, pre-synaptic vesicle endocytosis protein Synaptophysin, and vesicle release regulating protein Synapsin1 (Figures 1H and 1I). Last, we characterized hippocampal-dependent learning and memory in young and aged mice. Consistent with previous reports [31, 32], we detected age-related impairments in spatial memory using the radial arm water maze (RAWM) paradigm (Figures 1J and 1K; Data S1A), as well as impaired associative memory in contextual (Figure 1L), but not cued (Figure 1M), fear conditioning. No differences in baseline freezing or open-field activity were observed (Figures S1B and S1C). These data indicate age-related decreases in OGT and O-GlcNAc levels accompany neuronal and cognitive hallmarks of brain aging in the hippocampus.

Decreased Neuronal O-GlcNAcylation Elicits Aging-Associated Cellular Phenotypes in the Adult Hippocampus

We next assessed whether mimicking an age-related decrease in OGT and O-GlcNAcylation elicited features of brain aging. Specifically, to investigate the effects of decreased neuronal

Author Manuscript Author Manuscript Author Manuscript Author Manuscript

O-GlcNAcylation, we generated *Ogt*$^{flox/y}$ mice carrying an inducible *CamK2a-Cre-ER*^{T2} gene, in which *Ogt* is excised specifically in young adult forebrain neurons upon tamoxifen administration (Ogt-cKO mouse) (Figure 2A). We confirmed Ogt-cKO mice displayed decreased OGT and global protein O-GlcNAcylation in hippocampal lysates when compared to *Ogt*$^{flox/y}$ littermate controls (Figure S2A). Significant changes in expression were not detected outside of the forebrain in the cerebellum (Figure S2B). We assessed for gross hippocampal neurodegeneration using Nissl body staining, DAPI-mediated cell counts (Figure S2C), and immunohistological analysis for the apoptosis marker cleaved caspase 3, and no widespread cell loss or apoptosis were observed in Ogt-cKO or wild-type control mice (Figures 2B, 2E, and S2D).

Subsequently, we profiled aging-associated synaptic plasticity-related changes at the molecular and structural level in the hippocampi of Ogt-cKO mice using immunohistochemistry and Golgi analysis. We detected a decrease in neuronal pCREB in both CA1 and DG sub-regions and reduction in the number of activated neurons expressing cFos in the CA1 region of Ogt-cKO mice compared to control animals (Figures 2B-2D). Additionally, we examined whether Ogt-cKO mice displayed accompanying alterations in neuronal structure at the synaptic level using Golgi analysis. Acute loss of neuronal OGT resulted in a reduction in the number of tertiary dendritic spines on CA1 pyramidal neurons in Ogt-cKO mice (Figures 2F and 2G). Taken together, these *in vivo* data indicate that decreased O-GlcNAcylation in adult forebrain neurons recapitulates molecular and structural features observed during normal aging in the adult hippocampus.

Decreased Neuronal O-GlcNAcylation Alters Hippocampal Synaptic Protein Expression and Function

Next, we assessed expression of several synaptic markers in hippocampal lysates from Ogt-cKO or control mice. We observed a decrease in the protein levels of both NR2A and NR2B, an increase in the NR2A/NR2B ratio, as well as a decrease in PSD-95 and Synapsin1 in Ogt-cKO compared to control mice (Figures 3A and 3B). No differences were detected in Synaptophysin between genotypes (Figures 3A and 3B). Overall, Ogt-cKO mice display changes in synaptic protein expression indicative of altered synaptic function.

To expand upon these findings, we performed extracellular electrophysiological recordings of Schaffer collateral projections from CA3 to CA1 in hippocampal slices of Ogt-cKO and control mice (Figure 3C). We calculated the input-output relationship by plotting the amplitude of presynaptic volleys with the resulting slope of the evoked field excitatory post-synaptic potential (fEPSP) and detected no overall change in synaptic strength between Ogt-cKO and control mice (Figure 3D). We next measured paired-pulse ratio (PPR) to assess presynaptic release probability and did not observe a significant difference between control and Ogt-cKO mice (Figure 3E). These results suggest Ogt-cKO mice exhibit normal basal synaptic transmission from CA3 to CA1 compared to controls. While we observed no difference in LTD (Figures 3F and 3G), we did detect an increase in LTP in Ogt-cKO compared to control mice (Figures 3H and 3I) that was inversely correlated with hippocampal Ogt protein expression (Figure 3J). Collectively, these data indicate that

Author Manuscript Author Manuscript Author Manuscript Author Manuscript

decreased neuronal O-GlcNAcylation alters synaptic protein composition and excitatory synaptic function.

Decreased Neuronal O-GlcNAcylation Impairs Hippocampal-Dependent Learning and Memory

At a cognitive level, we profiled anxiety function using open field, and hippocampal-dependent learning and memory using RAWM and fear conditioning paradigms in Ogt-cKO and control mice (Figure 4A; Figure S3A). No differences in the time spent in the periphery or center of the open field were observed between genotypes during testing, indicative of normal general anxiety (Figure S3B). When testing spatial learning and memory using RAWM, all mice showed similar learning capacity during the training phase (Figure 4B). However, Ogt-cKO mice committed significantly more errors in locating the target platform during the testing phase compared to control animals (Figures 4B and 4C; Data S1B). During fear conditioning, Ogt-cKO mice exhibited elevated baseline freezing levels (Figure S3C), and when controlling for baseline freezing Ogt-cKO mice displayed decreased freezing during contextual and cued memory testing compared to controls (Figures 4D and 4E). These behavioral data indicate that loss of neuronal O-GlcNAcylation in adult mice elicits impairments in spatial learning and memory and associative fear memory.

Increased Neuronal O-GlcNAcylation in the Hippocampus Enhances Associative Fear Memory, but Not Spatial Learning and Memory, in Young Animals

Our findings indicate that decreasing neuronal O-GlcNAcylation mimics aspects of aging-associated cognitive impairments in the adult hippocampus. However, it remains an open question whether increasing O-GlcNAcylation in the adult hippocampus can enhance cognitive function. To test this possibility, we utilized a viral-mediated overexpression approach. We generated a lentivirus (LV) construct encoding OGT under the control of a neuron-specific Synapsin promoter. OGT overexpression and increased O-GlcNAcylation was confirmed *in vivo* in the hippocampus of adult wild-type mice stereotaxically injected LV encoding OGT (Figure S4).

Subsequently, young adult wild-type mice were then given bilateral stereotaxic injections of high-titer virus encoding OGT or GFP into their hippocampi and behaviorally tested following recovery using open-field, RAWM, and fear-conditioning paradigms (Figure 5A; Figure S5A). No differences in the time spent in the periphery or center of the open field were observed (Figure S5B). All mice showed similar learning capacity during the training phase of the RAWM (Figure 5B), and no differences in the number of errors in locating the target platform were observed during learning and memory testing (Figures 5B and 5C; Data S1C). During fear conditioning, no differences in baseline freezing time were detected (Figure S5C). However, mice with increased neuronal expression of OGT exhibited increased freezing time during contextual (Figure 5D), but not cued (Figure 5E), memory testing. The data indicate that increased neuronal O-GlcNAcylation in the adult hippocampus is sufficient to enhance associative fear memory, but not spatial learning and memory, in young adult mice.

Author Manuscript Author Manuscript Author Manuscript Author Manuscript

Increased Neuronal O-GlcNAcylation in the Hippocampus Ameliorates Impairments in Spatial Learning and Memory and Associative Fear Memory in Aged Animals

Last, we investigated the potential of increasing neuronal O-GlcNAcylation in the aged hippocampus to rescue age-related cognitive impairments. Aged animals were given bilateral stereotaxic injections of high-titer LV encoding OGT or GFP under the Synapsin promoter into the hippocampus and behaviorally tested following recovery using open field and RAWM or fear-conditioning paradigms, respectively (Figure 6A; Figure S6A). No differences in the time spent in the periphery or center of the open field were observed (Figure S6B). When testing spatial learning and memory using RAWM, all mice showed similar learning capacity during the training phase (Figure 6B). However, aged mice with increased neuronal OGT expression committed significantly less errors in locating the target platform during the learning and memory testing phase compared to control aged animals (Figures 6B and 6C; Data S1D). During fear-conditioning training mice exhibited no differences in baseline freezing time (Figure S6C). However, aged mice with increased neuronal OGT expression exhibited increased freezing time during contextual (Figure 6D), but not cued (Figure 6E), memory testing. Additionally, a naive young adult control group was included, and age-related cognitive impairments were corroborated in control aged animals (Figures 6B-6E). These behavioral data indicate that increased neuronal OGT expression in the aged hippocampus is sufficient to rescue, in part, age-related cognitive impairments, positing increased O-GlcNAcylation as a valuable molecular target for cognitive rejuvenation.

DISCUSSION

Cumulatively, our data frame O-GIcNAc as a neuroprotective post-translational protein modification, whose age-related decline promotes neuronal and cognitive impairments that increase susceptibility to subsequent neurodegenerative phenotypes. Our genetic knockout and *in vivo* overexpression data demonstrate that modulating O-GlcNAcylation in the adult brain, by targeting neuronal OGT, can bi-directionally regulate hippocampal-dependent cognitive function in young adult animals. Moreover, we demonstrate that increasing neuronal OGT in the aged hippocampus is sufficient to rescue, in part, age-related impairments in hippocampal-dependent cognitive processes. Ultimately, our data identify O-GlcNAcylaton as a key molecular mediator promoting cognitive rejuvenation.

In addition to aging-associated hallmarks, we did observe some alterations in Ogt-cKO mice not classically observed in the aged brain, mainly a decrease in synaptic PSD-95 and Synapsin-1 expression alongside increased LTP. While increased LTP is often assumed to be a correlate for cognitive enhancement, it has also been reported by independent groups in the presence of cognitive impairments [33-35]—suggesting the relationship between LTP and memory is more complex than previously appreciated. In line with this, we detected impairments in both hippocampal-dependent spatial learning and memory, as well as associative fear memory in Ogt-cKO mice despite observing an increase in hippocampal LTP.

Previous work using a non-inducible conditional OGT knockout mouse model, in which neuronal *Ogt* is excised during post-natal development, reported gross neurodegeneration

Author Manuscript Author Manuscript Author Manuscript Author Manuscript

and cell death in the adult hippocampus after extended loss of neuronal OGT [8]. By contrast, we demonstrate that mimicking an age-related decline in O-GlcNAcylation in adult mice by utilizing a temporally controlled neuronal *Ogt* knockout mouse model recapitulates a surprising number of aging-associated neuronal and cognitive impairments in the absence of neurodegeneration. Our findings are consistent with complementary studies reporting no cell death in the adult brain after acute loss of neuronal O-GlcNAcylation, although investigations were predominantly focused on the hypothalamus [36]. Collectively, these studies begin to provide temporal resolution between the more acute effects of decreased O-GlcNAcylation in regulating synaptic plasticity-related phenotypes versus the more chronic effects on neurodegeneration. These findings also reflect the initial emergence of synaptic plasticity-related impairments observed during normal aging that are followed long term by neuronal loss in age-related neurodegenerative conditions, such as Alzheimer's disease.

Differences in decreased O-GlcNAc levels exist between the brains of normal aged individuals and Alzheimer's disease patients, suggesting that the magnitude of this decline may differentially regulate aging-associated versus neurodegenerative phenotypes. In addition to differences in overall O-GlcNAc levels, differential expression of distinct OGT isoforms may likewise represent complementary mechanisms selectively governing normal brain aging and onset of neurodegenerative conditions. In mammals, both a full-length OGT isoform (ncOGT) and a short OGT isoform (sOGT) are present in the nucleus and cytoplasm and differ only in their protein-protein interaction domains. Although ncOGT is more catalytically active, each isoform is believed to have a degree of protein recognition specificity [37, 38]. In the adult mammalian brain ncOGT and sOGT are highly expressed in the hippocampus, with expression of ncOGT selectively decreasing during aging [23]. It is necessary for future studies to begin to delineate how specificity for protein O-GlcNAcylation by the different OGT isoforms may regulate aging-associated versus neurodegenerative neuronal phenotypes through distinct molecular mechanisms. While proteomics analysis at the synaptic level has revealed high levels of O-GlcNAcylation in the hippocampus of young adult mice [12, 14, 15, 17], no such comparative studies exist in the context of physiological aging and Alzheimer's disease.

From a translational perspective, mounting evidence in animal models indicates potential for rejuvenation of cellular and cognitive functions in the aging brain [25-29, 39, 40]. However, the ability to utilize this potential is predicated on identifying molecular targets that reverse the effects of aging in vulnerable regions of the brain, such as the hippocampus. Our behavioral data in young adult and aged mice posit increased O-GlcNAcylation as a key molecular mediator promoting cognitive rejuvenation. Indeed, increasing OGT in the aged hippocampus was sufficient to ameliorate age-related impairments in learning and memory. Given the emerging beneficial attributes ascribed to O-GlcNAcylation, significant therapeutic potential exists with respect to developing interventions that target post-translational protein modifications to enhance cognition, reverse brain aging, and consequently circumvent onset of age-related neurodegenerative diseases. Interestingly, in *C. elegans* increasing O-GlcNAcylation has been reported to extend lifespan [20], raising the tantalizing possibility that O-GlcNAcylation-mediated rejuvenation may extend beyond the brain to broad tissue types at the organismal level.

Author Manuscript Author Manuscript Author Manuscript Author Manuscript

STAR★METHODS

LEAD CONTACT AND MATERIALS AVAILABILITY

Further information and requests for resources and reagents should be directed to and will be fulfilled by the Lead Contact, Saul Villeda (saul.villeda@ucsf.edu). Plasmids generated in this study have not been deposited on an external repository but are available for distribution on request from the Lead Contact.

EXPERIMENTAL MODEL AND SUBJECT DETAILS

Animal Models—The following mouse lines were used: C57BL/6J mice (Jackson Laboratory line 000664), *Ogt*$^{flox/y}$ mice (The Jackson Laboratory line 004860), and *CamK2a-CreER*^{T2} (Jackson Laboratory line 012362). All mice used were on a C57BL/6 genetic background. All studies were done in young (2-3 months) or aged (18-22 months) male mice, and were not involved in any previous procedures. The numbers of mice used to result in statistically significant differences were calculated using standard power calculations with a = 0.05 and a power of 0.8. We used an online tool (https://www.stat.uiowa.edu/~rlenth/Power/index.html) to calculate power and samples size based on experience with the respective tests, variability of the assays and inter-individual differences within groups. Mice were housed under specific pathogen-free conditions under a 12-h light-dark cycle, and all animal handling and use was in accordance with institutional guidelines approved by the University of California San Francisco Institutional Animal Care and Use Committee (IACUC) and the Stanford University Administrative Panel on Laboratory Animal Care (APLAC).

METHOD DETAILS

PCR Genotyping—Ogt floxed and Camk2a-CreERT2 alleles were genotyped from skin biopsies using PCR with Ogt primers and Camk2a-CreERT2. Primers specific for the Myogenin gene were included in the reaction as a control. Ogt floxed forward primer: CATCTCTCCAGCCC CACAAACTG. Ogt floxed reverse primer: GACGAAGCAGGAGGGGAGAGCAC. Primer Cre forward: AGCTCGTCAATCAAGCTGGT. Primer Cre reverse: CAGGTTCTTGCGAACCTCAT. Myogenin forward primer: TTACGTCCATCGTGGACAGC. Myogenin reverse primer: TGGGCTGGGTGTTAGCCTTA.

Tamoxifen injections—Animals were injected via intraperitoneal injection with 180mg/kg of tamoxifen or vehicle once every 24 h for a total of 5 injections per animal. Animals were monitored after recovery and five weeks allowed to pass after the final injection before any analyses were performed.

Stereotaxic injections—Animals were placed in a stereotaxic frame and anesthetized with 2% isoflurane (2L/min oxygen flow rate) delivered through an anesthesia nose cone. Ophthalmic eye ointment was applied to the cornea to prevent desiccation during surgery. The area around the incision was trimmed. Viral solutions were injected bilaterally into the dorsal hippocampi using the following coordinates: (from bregma) anterior = −2mm, lateral = 1.5mm, (from skull surface) height = −2.1mm. 2 μL volume was injected stereotaxically

Author Manuscript Author Manuscript Author Manuscript Author Manuscript

over 10 min (injection speed: 0.20 μl/min) using a 10 μL 26 s gauge Hamilton syringe. To limit reflux along the injection track, the needle was maintained *in situ* for three min, slowly pulled out half way and kept in position for an additional two min. The skin was closed using silk suture. Each mouse was injected subcutaneously with the analgesic Bupranex. Mice were single-housed and monitored during recovery.

Radial Arm Water Maze—Spatial learning and memory was assessed using the RAWM paradigm [41]. In this task the goal arm location containing a platform remains constant throughout the training and testing phase, while the start arm is changed during each trial. Entry into an incorrect arm is scored as an error, and errors are averaged over training blocks (three consecutive trials). On day one during the training phase, mice are trained for 15 trials, with trials alternating between a visible and hidden platform. Every 3 trials are counted as one block of training. Prior to the final 3 trials of day 1 (block 5), the mice are given an extended break, and short-term memory is then tested using three consecutive hidden platform trials. On day 2 during the testing phase, mice are tested for 15 trials per day with a hidden platform. All behavior is performed double blinded.

Contextual Fear Conditioning—Associative fear memory was assessed using contextual and cued fear conditioning paradigms [32]. In this task mice learned to associate the environmental context (fear conditioning chamber) with an aversive stimulus (mild foot shock; unconditioned stimulus, US) enabling testing for hippocampal-dependent contextual fear conditioning. The mild foot shock was paired with a light and tone cue (conditioned stimulus, CS) in order to also assess amygdala- dependent cued fear conditioning. Conditioned fear was displayed as freezing behavior. Specific training parameters are as follows: tone duration is 30 s; level is 70 dB, 2 kHz; shock duration is 2 s; intensity is 0.6 mA. On day 1 each mouse was placed in a fear-conditioning chamber and allowed to explore for 2 min before delivery of a 30 s tone (70 dB) ending with a 2 s foot shock (0.6mA). Two min later, a second CS-US pair was delivered. On day 2 each mouse was first place in the fear- conditioning chamber containing the same exact context, but with no administration of a CS or foot shock. Freezing was analyzed for 1-3 min. One h later, the mice were placed in a new context containing a different odor, cleaning solution, floor texture, chamber walls and shape. Animals were allowed to explore for 2 min before being re-exposed to the CS. Freezing was analyzed for 1-3 min. Freezing was measured using a FreezeScan video tracking system and software (Clever Sys). All behavior is performed double blinded.

Open Field—Mice were placed in the center of an open 40cm × 40cm square chamber (Kinder Scientific) with no cues or stimuli and allowed to move freely ofr 10 min. Infrared photobeam breaks were recorded and movement metrics analyzed by MotorMonitor software (Kinder Scientific).

Western Blot Analysis—Mouse brain tissues were dissected after perfusion of animal and snap frozen and lysed in RIPA lysis buffer (500 mM Tris, pH 7.4, 150 mM NaCl, 0.5% Na deoxycholate, 1% NP40, 0.1% SDS, complete protease inhibitors 2X; Roche, and PUGNAc 100uM; Sigma). Tissue lysates were mixed with 4x NuPage LDS loading buffer (Invitrogen), loaded on a 4%–12% SDS polyacrylamide gradient gel (Invitrogen), and

Author Manuscript Author Manuscript Author Manuscript Author Manuscript

subsequently transferred onto a nitrocellulose membrane. The blots were blocked in 5% milk in Tris-Buffered Saline with Tween (TBST) and incubated with mouse anti-O-GlcNAc antibody (RL2) ab2739 (1:500, Abcam), rabbit anti-OGT antibody (H-300) sc-32921 (1:1000, SC Biotech), rabbit anti-PSD-95 antibody #2507 (1:300; CS Technology), rabbit anti-NR2B ab65783 (1:1000, Abcam), rabbit anti-synapsin-1 ab18814 (1:1000, Abcam), mouse anti-synaptophysin (SY38) MAB5258 (1:1000, EMD Millipore), and mouse anti-GAPDH (6C5) ab8245 (1:10,000, Abcam). Horseradish peroxidase-conjugated secondary antibodies and an ECL kit (Clarity ECL, Bio-Rad) were used to detect protein signals. Multiple exposures were taken to select images within the dynamic range of the film. Selected films were scanned (300 dpi) and quantified using FIJI software (Version 1.0). GAPDH bands were used for normalization.

Immunohistochemistry—Tissue processing and immunohistochemistry was performed on free-floating sections. Mice were anesthetized with ketamine, transcardially perfused with 0.9% saline, and brains removed and fixed in phosphate-buffered 4% paraformaldehyde for 48h before cryprotection with 30% sucrose. Free floating coronal sections (40 mm) were incubated overnight with either rabbit anti-phospho CREB (Ser133) 06-519 (1:1000; EMD Millipore), rabbit anti-Cleaved Caspase-3 (Asp175) antibody #9661 (1:400; CS Technology) or rabbit anti-c-Fos (Ab-5) (4-17) (1:10,000; Calbiochem) primary antibodies, and staining was revealed using biotinylated secondary antibodies and the ABC kit (Vector) with Diaminobenzidine (DAB, Sigma-Aldrich). Sections were mounted in phosphate buffer on superfrost plus microscope slides (ThermoFisher), allowed to dry overnight, briefly soaked in Citrisolv and coverslipped with Entellan. Individual cell number was quantified for c-Fos or cleaved caspase 3 using FIJI software (Version 1.0).

Nissl Staining—Sections were cut to 40 mm and mounted on superfrost plus microscope slides (ThermoFisher) and allowed to dry overnight. Slides were then soaked in 100% ethanol 3×2min each, and then immersed in Cresyl Violet (Sigma Aldrich) working solution for 10 min. Slides were then dipped in 95% ethanol, soaked in 100% ethanol 2×2min, then in Citrasolv 2×2min before being coverslipped with Entellan. Mean intensity was quantified using FIJI software (Version 1.0).

Golgi Staining—After brain removal, hemispheres were immersed in 10 mL of A+B solution from FD Rapid GolgiStain Kit, which was prepared 24 h prior. Solution was then changed after the initial 12 h and left for 10 days at room temperature in the dark. Brains were then transferred to solution C, which was changed after the initial 24 h, and then left for 3 days at room temperature in the dark. Brains were cut into 100 mm sections using a vibratome and were mounted onto slides coated with 0.3% gelatin in solution C. Slides were then air-dried for 24 h in the dark. Slides were immersed into Milli-Q H_2O, 2 × 4 min with gentle shaking, then transferred to a developing solution (Solution D, E, and Milli-Q H_2O) for 10 min. Slides were then rinsed 2×4 min in Milli-Q H_2O, dehydrated through graded ethanol, immersed in Xylenes 3×4 min, and then coverslipped using Permount. All slides were then blinded and neurons imaged using a 63X oil immersion objective. Tertiary dendritic spine density was quantified using FIJI software (Version 1.0) for dendritic tracing and spine count, and results were un-blinded just prior to statistical analyses.

Author Manuscript Author Manuscript Author Manuscript Author Manuscript

Slice Electrophysiology—Coronal brain slices (300 mm) containing hippocampus were prepared from 8-10 week old WT and OGT cKO littermate mice. Mice were anesthetized with isoflurane, decapitated, and the brain was quickly removed and transferred to ice-cold artificial cerebrospinal fluid (ACSF) containing 125 mM NaCl, 2.5 mM KCl, 1.25 mM NaH2PO4, 25 mM NaHCO3, 15 mM glucose, 2 mM CaCl2, and 1 mM MgCl2, oxygenated with 95% O2 and 5% CO2 (300-305 mOsm, pH 7.4). Acute brain slices containing hippocampus were cut with a vibratome (VT1200S, Leica) and transferred to an incubation chamber containing ACSF at 34°C for 30 min and then to a recovery chamber containing ACSF at room temperature for 30 min. Before recording, coronal slices were hemisected and hippocampi dissected before being transferred to a submerged recording chamber perfused with ACSF at a rate of 2~3 mL/min at 30°C. Brain slices were recorded within 4 h after recovery. CA1 field potential were evoked by Schaffer collateral electrical stimulation, recorded using broken tip borosilicate glass pipettes filled with ACSF. Signals were acquired using a Multiclamp 700B, filtered at 2kHz, and digitized at 10 kHz. After recording a stable baseline for at least 20 min, LTP was induced by 20 hz presentation of 4 trains (each consisting of 10 pulses at 100 hz), and LTD by a single-pulse, low-frequency stimulation (SP-LFS) (900 pulses at 1 hz). Recorded data were monitored online using WinLTP and WinWCP and analyzed offline using MATLAB and Prism.

Viral plasmids and generation of lentiviral particles—RNA was isolated from adult mouse hippocampal tissue using TRIZol reagent (Thermo Fisher Scientific) and PureLink RNA Mini Kit following the manufacturer's instructions. The RNA concentration was determined via Nanodrop and RNA was reverse transcribed using the High-Capacity cDNA Reverse Transcription Kit (Thermo Fisher Scientific) and oligo dT primers (Promega). The following primers were used for PCR amplification of the Ogt coding sequence and partial 3' and 5' untranslated regions (UTRs) from mouse hippocampal cDNA: CACCGTTCAGTATTCTGTGCCGCC (forward primer); TAGGGCAATTCTCCTGTGCG (reverse primer). The Ogt ORF was cloned into the pENTR D-TOPO vector (ThermoFisher Scientific, Cat# K240020) and sequence verified using the following primers: M13F, M13R, CAACCAAACTTTGCAGTAGCCTGG, AAGCTGCAGGAAGCACTGATG, ACACCTTATGCAGTCTAT TCCAGGC, ACAATCCAGACAG CAGTAACACAGC. The coding sequence was further amplified and cloned into a lentiviral expression plasmid containing a Synapsin promoter using the restriction sites NheI and BamHI. A Synapsin GFP construct, based on the same lentiviral backbone, was used as a control. All coding plasmid sequences were verified by Sanger sequencing. Endotoxin free plasmid kits were used for plasmid preparation prior to in virus production and *in vivo* use. Overexpression quality was tested with western blot analysis. Preparation of non-replicative lentiviral particles was performed using the UCSF Viracore, and titered to 1.0×10^9 viral particles/ml.

QUANTIFICATION AND STATISTICAL ANALYSIS

All experiments were randomized and blinded by an independent researcher. Researchers remained blinded throughout histological, molecular, and behavioral assessments. Groups were un-blinded at the end of each experiment upon statistical analysis. Graphed data are expressed as mean ± SEM. Statistical analysis was performed with Prism 5.0 software (GraphPad Software). Means between two groups were compared with two-tailed, unpaired

Author Manuscript Author Manuscript Author Manuscript Author Manuscript

Student's t test. Comparisons of means from multiple groups with each other or against one control group were analyzed with one-way ANOVA and Tukey's post hoc test. For RAWM behavioral data, trial by group interactions is analyzed with repeated-measures ANOVA and Bonferroni post hoc test (Data S1). All histology, electrophysiology and behavior experiments conducted were done in a randomized and blinded fashion. For each experiment, the overall size of the experimental groups corresponded to distinct animals. Unique samples were not measured repeatedly within the same characterization of a given cohort.

DATA AND CODE AVAILABILITY

This study did not generate or analyze datasets or code.

Supplementary Material

Refer to Web version on PubMed Central for supplementary material.

ACKNOWLEDGMENTS

We thank Dr. Susan Fisher for insightful comments. This work was funded by NIH Ruth L. Krischstein NRSA predoctoral fellowship (E.G.W., F31-AG050415), HHMI Gilliam Fellowship (E.A.), NSF GRFP (E.A.), NINDS/NIH NS091144 (J.B.D.), GG Network endowed research fund (J.B.D.), NIA (R01 AG053382, RF1 AG062357), and a gift from Marc and Lynne Benioff (S.A.V.).

REFERENCES

1. Hedden T, and Gabrieli JD (2004). Insights into the ageing mind: a view from cognitive neuroscience. Nat. Rev. Neurosci. 5, 87–96. [PubMed: 14735112]
2. Mattson MP, and Magnus T (2006). Ageing and neuronal vulnerability. Nat. Rev. Neurosci. 7, 278–294. [PubMed: 16552414]
3. Andrews-Hanna JR, Snyder AZ, Vincent JL, Lustig C, Head D, Raichle ME, and Buckner RL (2007). Disruption of large-scale brain systems in advanced aging. Neuron 56, 924–935. [PubMed: 18054866]
4. Bishop NA, Lu T, and Yankner BA (2010). Neural mechanisms of ageing and cognitive decline. Nature 464, 529–535. [PubMed: 20336135]
5. Morrison JH, and Baxter MG (2012). The ageing cortical synapse: hallmarks and implications for cognitive decline. Nat. Rev. Neurosci. 13, 240–250. [PubMed: 22395804]
6. Yuzwa SA, and Vocadlo DJ (2014). O-GlcNAc and neurodegeneration: biochemical mechanisms and potential roles in Alzheimer's disease and beyond. Chem. Soc. Rev. 43, 6839–6858. [PubMed: 24759912]
7. Lagerlöf O, and Hart GW (2014). O-GlcNAcylation of neuronal proteins: roles in neuronal functions and in neurodegeneration. Adv. Neurobiol. 9, 343–366. [PubMed: 25151387]
8. Wang AC, Jensen EH, Rexach JE, Vinters HV, and Hsieh-Wilson LC (2016). Loss of O-GlcNAc glycosylation in forebrain excitatory neurons induces neurodegeneration. Proc. Natl. Acad. Sci. USA 113, 15120–15125. [PubMed: 27956640]
9. Banerjee PS, Lagerlöf O, and Hart GW (2016). Roles of O-GlcNAc in chronic diseases of aging. Mol. Aspects Med. 51, 1–15. [PubMed: 27259471]
10. Ma X, Li H, He Y, and Hao J (2017). The emerging link between O-GlcNAcylation and neurological disorders. Cell. Mol. Life Sci. 74, 3667–3686. [PubMed: 28534084]
11. Lagerlöf O (2018). O-GlcNAc cycling in the developing, adult and geriatric brain. J. Bioenerg. Biomembr. 50, 241–261. [PubMed: 29790000]

Author Manuscript Author Manuscript Author Manuscript Author Manuscript

12. Vosseller K, Trinidad JC, Chalkley RJ, Specht CG, Thalhammer A, Lynn AJ, Snedecor JO, Guan S, Medzihradszky KF, Maltby DA, et al. (2006). O-linked N-acetylglucosamine proteomics of postsynaptic density preparations using lectin weak affinity chromatography and mass spectrometry. Mol. Cell. Proteomics 5, 923–934. [PubMed: 16452088]
13. Tallent MK, Varghis N, Skorobogatko Y, Hernandez-Cuebas L, Whelan K, Vocadlo DJ, and Vosseller K (2009). In vivo modulation of O-GlcNAc levels regulates hippocampal synaptic plasticity through interplay with phosphorylation. J. Biol. Chem. 284, 174–181. [PubMed: 19004831]
14. Alfaro JF, Gong CX, Monroe ME, Aldrich JT, Clauss TR, Purvine SO, Wang Z, Camp DG 2nd, Shabanowitz J, Stanley P, et al. (2012). Tandem mass spectrometry identifies many mouse brain O-GlcNAcylated proteins including EGF domain-specific O-GlcNAc transferase targets. Proc. Natl. Acad. Sci. USA 109, 7280–7285. [PubMed: 22517741]
15. Trinidad JC, Barkan DT, Gulledge BF, Thalhammer A, Sali A, Schoepfer R, and Burlingame AL (2012). Global identification and characterization of both O-GlcNAcylation and phosphorylation at the murine synapse. Mol. Cell. Proteomics 11, 215–229. [PubMed: 22645316]
16. Rexach JE, Clark PM, Mason DE, Neve RL, Peters EC, and Hsieh-Wilson LC (2012). Dynamic O-GlcNAc modification regulates CREB-mediated gene expression and memory formation. Nat. Chem. Biol. 8, 253–261. [PubMed: 22267118]
17. Trinidad JC, Schoepfer R, Burlingame AL, and Medzihradszky KF (2013). N- and O-glycosylation in the murine synaptosome. Mol. Cell. Proteomics 12, 3474–3488. [PubMed: 23816992]
18. Taylor EW, Wang K, Nelson AR, Bredemann TM, Fraser KB, Clinton SM, Puckett R, Marchase RB, Chatham JC, and McMahon LL (2014). O-GlcNAcylation of AMPA receptor GluA2 is associated with a novel form of long-term depression at hippocampal synapses. J. Neurosci. 34, 10–21. [PubMed: 24381264]
19. Lagerlöf O, Hart GW, and Huganir RL (2017). O-GlcNAc transferase regulates excitatory synapse maturity. Proc. Natl. Acad. Sci. USA 114, 1684–1689. [PubMed: 28143929]
20. Rahman MM, Stuchlick O, El-Karim EG, Stuart R, Kipreos ET, and Wells L (2010). Intracellular protein glycosylation modulates insulin mediated lifespan in C.elegans. Aging (Albany N.Y.) 2, 678–690.
21. Love DC, Ghosh S, Mondoux MA, Fukushige T, Wang P, Wilson MA, Iser WB, Wolkow CA, Krause MW, and Hanover JA (2010). Dynamic O-GlcNAc cycling at promoters of Caenorhabditis elegans genes regulating longevity, stress, and immunity. Proc. Natl. Acad. Sci. USA 107, 7413–7418. [PubMed: 20368426]
22. O'Donnell N, Zachara NE, Hart GW, and Marth JD (2004). Ogtdependent X-chromosome-linked protein glycosylation is a requisite modification in somatic cell function and embryo viability. Mol. Cell. Biol. 24,1680–1690. [PubMed: 14749383]
23. Liu Y, Li X, Yu Y, Shi J, Liang Z, Run X, Li Y, Dai CL, Grundke-Iqbal I, Iqbal K, et al. (2012). Developmental regulation of protein O-GlcNAcylation, O-GlcNAc transferase, and O-GlcNAcase in mammalian brain. PLoS ONE 7, e43724. [PubMed: 22928023]
24. Liu F, Shi J, Tanimukai H, Gu J, Gu J, Grundke-Iqbal I, Iqbal K, and Gong CX (2009). Reduced O-GlcNAcylation links lower brain glucose metabolism and tau pathology in Alzheimer's disease. Brain 132, 1820–1832. [PubMed: 19451179]
25. Fan X, Wheatley EG, and Villeda SA (2017). Mechanisms of Hippocampal Aging and the Potential for Rejuvenation. Annu. Rev. Neurosci. 40, 251–272. [PubMed: 28441118]
26. Villeda SA, Plambeck KE, Middeldorp J, Castellano JM, Mosher KI, Luo J, Smith LK, Bieri G, Lin K, Berdnik D, et al. (2014). Young blood reverses age-related impairments in cognitive function and synaptic plasticity in mice. Nat. Med. 20, 659–663. [PubMed: 24793238]
27. Khrimian L, Obri A, Ramos-Brossier M, Rousseaud A, Moriceau S, Nicot AS, Mera P, Kosmidis S, Karnavas T, Saudou F, et al. (2017). Gpr158 mediates osteocalcin's regulation of cognition. J. Exp. Med. 214, 2859–2873. [PubMed: 28851741]
28. Castellano JM, Mosher KI, Abbey RJ, McBride AA, James ML, Berdnik D, Shen JC, Zou B, Xie XS, Tingle M, et al. (2017). Human umbilical cord plasma proteins revitalize hippocampal function in aged mice. Nature 544, 488–492. [PubMed: 28424512]

Author Manuscript Author Manuscript Author Manuscript Author Manuscript

29. Yu XW, Curlik DM, Oh MM, Yin JC, and Disterhoft JF (2017). CREB overexpression in dorsal CA1 ameliorates long-term memory deficits in aged rats. eLife 6, w19358.

30. Massey PV, Johnson BE, Moult PR, Auberson YP, Brown MW, Molnar E, Collingridge GL, and Bashir ZI (2004). Differential roles of NR2A and NR2B-containing NMDA receptors in cortical long-term potentiation and long-term depression. J. Neurosci. 24, 7821–7828. [PubMed: 15356193]

31. Villeda SA, Luo J, Mosher KI, Zou B, Britschgi M, Bieri G, Stan TM, Fainberg N, Ding Z, Eggel A, et al. (2011). The ageing systemic milieu negatively regulates neurogenesis and cognitive function. Nature 477, 90–94. [PubMed: 21886162]

32. Smith LK, He Y, Park JS, Bieri G, Snethlage CE, Lin K, Gontier G, Wabl R, Plambeck KE, Udeochu J, et al. (2015). b2-microglobulin is a systemic pro-aging factor that impairs cognitive function and neurogenesis. Nat. Med. 21, 932–937. [PubMed: 26147761]

33. Migaud M, Charlesworth P, Dempster M, Webster LC, Watabe AM, Makhinson M, He Y, Ramsay MF, Morris RG, Morrison JH, et al. (1998). Enhanced long-term potentiation and impaired learning in micewith mutant postsynaptic density-95 protein. Nature 396, 433–439. [PubMed: 9853749]

34. Gu Y, Mcllwain KL, Weeber EJ, Yamagata T, Xu B, Antalffy BA, Reyes C, Yuva-Paylor L, Armstrong D, Zoghbi H, et al. (2002). Impaired conditioned fear and enhanced long-term potentiation in Fmr2 knock-out mice. J. Neurosci. 22, 2753–2763. [PubMed: 11923441]

35. Kim MH, Choi J, Yang J, Chung W, Kim JH, Paik SK, Kim K, Han S, Won H, Bae YS, et al. (2009). Enhanced NMDA receptor-mediated synaptic transmission, enhanced long-term potentiation, and impaired learning and memory in mice lacking IRSp53. J. Neurosci. 29, 1586–1595. [PubMed: 19193906]

36. Lagerlöf O, Slocomb JE, Hong I, Aponte Y, Blackshaw S, Hart GW, and Huganir RL (2016). The nutrient sensor OGT in PVN neurons regulates feeding. Science 351, 1293–1296. [PubMed: 26989246]

37. Riu IH, Shin IS, and Do SI (2008). Sp1 modulates ncOGT activity to alter target recognition and enhanced thermotolerance in E. coli. Biochem. Biophys. Res. Commun. 372, 203–209. [PubMed: 18486602]

38. Lazarus BD, Love DC, and Hanover JA (2006). Recombinant O-GlcNAc transferase isoforms: identification of O-GlcNAcase, yes tyrosine kinase, and tau as isoform-specific substrates. Glycobiology 16, 415–421. [PubMed: 16434389]

39. Katsimpardi L, Litterman NK, Schein PA, Miller CM, Loffredo FS, Wojtkiewicz GR, Chen JW, Lee RT, Wagers AJ, and Rubin LL (2014). Vascular and neurogenic rejuvenation of the aging mouse brain by young systemic factors. Science 344, 630–634. [PubMed: 24797482]

40. Gontier G, Iyer M, Shea JM, Bieri G, Wheatley EG, Ramalho-Santos M, and Villeda SA (2018). Tet2 Rescues Age-Related Regenerative Decline and Enhances Cognitive Function in the Adult Mouse Brain. Cell Rep. 22, 1974–1981. [PubMed: 29466726]

41. Alamed J, Wilcock DM, Diamond DM, Gordon MN, and Morgan D (2006). Two-day radial-arm water maze learning and memory task; robust resolution of amyloid-related memory deficits in transgenic mice. Nat. Protoc. 1, 1671–1679. [PubMed: 17487150]

Author Manuscript Author Manuscript Author Manuscript Author Manuscript

Highlights

- Decreased hippocampal OGT and O-GlcNAcylation accompany neuronal hallmarks of aging
- Decreasing neuronal OGT in the young hippocampus impairs plasticity and cognition
- Increasing neuronal OGT in the young hippocampus enhances cognition
- Restoring neuronal OGT in the aged hippocampus rescues cognitive impairments

Author Manuscript
Author Manuscript
Author Manuscript
Author Manuscript

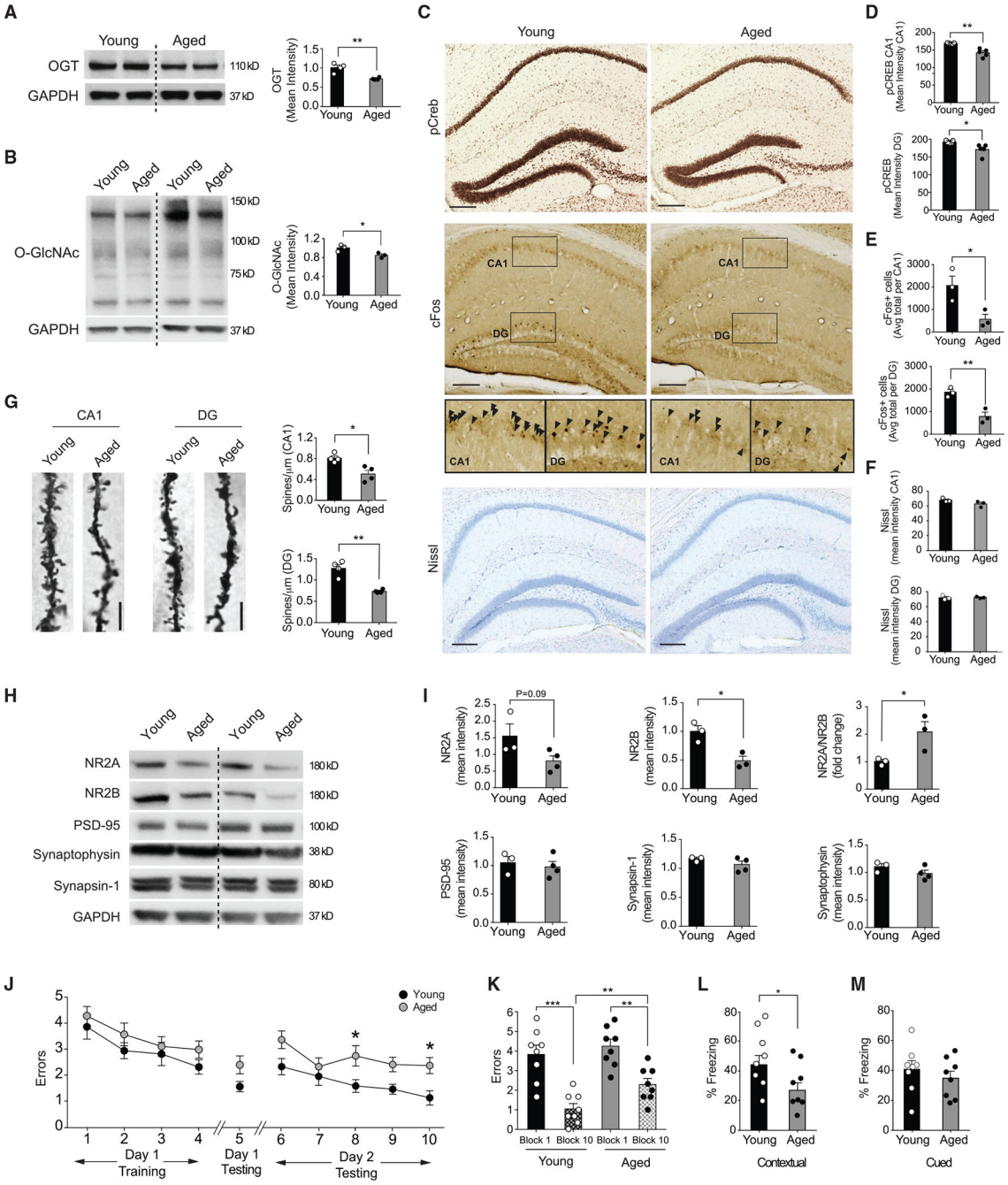

Figure 1. OGT Expression and O-GlcNAcylation Decreases in the Aged Hippocampus Coincident with Synaptic and Cognitive Impairments

(A) Representative western blot of OGT protein from whole hippocampal lysates of young (3 months) and aged (18–22 months) mice. Quantification represented as mean optical intensity normalized to GAPDH. n = 4 mice per group.

(B) Representative western blot of O-GlcNAc levels from whole hippocampal lysates of young (3 months) and aged (18–22 months) mice. Quantification represented as mean optical intensity normalized to GAPDH. n = 3 mice per group.

Author Manuscript Author Manuscript Author Manuscript Author Manuscript

(C) Representative images of phosphorylated CREB (pCREB) and cFos immunostain and Nissl stain in the hippocampus of young (3 months) and aged (18 months) mice. Scale bar, 200 mm. See also Figure S1.
(D) Quantification of pCREB immunostain mean intensity in the CA1 and dentate gyrus (DG) regions of the hippocampus, n = 5 mice per group.
(E) Quantification of cFos-positive cells in the CA1 and DG regions of the hippocampus, n = 3 mice per group.
(F) Quantification of Nissl stain mean intensity in the CA1 and DG regions of the hippocampus, n = 3 mice per group. See also Figure S1.
(G) Representative field of Golgi stain from CA1 pyramidal neurons and DG granule cell neurons in young (3 months) versus aged (24 months) mice. Quantification of spine number from tertiary dendrites, n = 4 neurons per mouse and 4 mice per group.
(H) Representative western blot of synaptic proteins NR2A, NR2B PSD-95, Synaptophysin, and Synapsin-1 from whole hippocampal lysates of young (3 months) and aged (24 months) mice.
(I) Quantification of synaptic protein expression from whole hippocampal lysates represented as mean optical intensity normalized to GAPDH. n = 3 mice per group.
(J and K) Hippocampal-dependent spatial learning and memory was assessed in young (3 months) and aged (18–20 s) mice using radial arm water maze (RAWM. Quantification of the number of entry errors during RAWM training (J) and testing (J and K). See also Data S1.
(L and M) Associative fear memory was assessed in young (3 months) and aged (18–20 months) mice using contextual (L) and cued (M) fear conditioning. Quantification of percentage of freezing 24 h after training; n = 8 mice per group. See also Figure S1.
Data are represented as mean ± SEM; *p < 0.05; **p < 0.01; ***p < 0.001; ****p < 0.0001; repeated-measures ANOVA, Bonferroni post hoc test (K); one-way ANOVA, Tukey’s post hoc test (K), t test (A, B, D–F, I, L, and M).

Author Manuscript
Author Manuscript
Author Manuscript
Author Manuscript

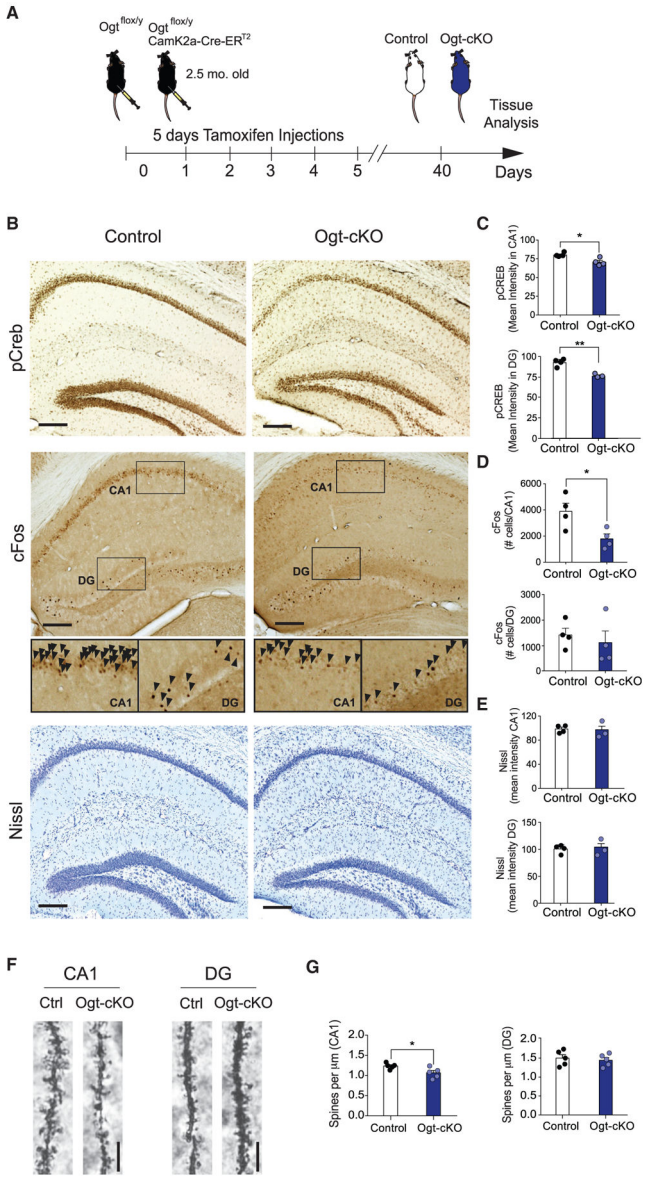

Figure 2. Abrogation of OGT in the Adult Brain Elicits Aging-Associated Neuronal Phenotypes in the Hippocampus

(A) Schematic depicting the timeline for the generation of and subsequent experiments using the conditional excitatory neuron Ogt knockout (Ogt-cKO) and control mouse. See also Figure S2.

(B) Representative images of phosphorylated CREB (pCREB) and cFos immunostain and Nissl stain in the hippocampus of young Ogt-cKO and control mice. Scale bar, 200 mm. See also Figure S2.

(C) Quantification of pCREB immunostain mean intensity in CA1 and DG regions of the hippocampus, n = 4 mice per group.

(D) Quantification of cFos-positive cells in the CA1 and DG regions of the hippocampus, n = 4 mice per group.

Author Manuscript Author Manuscript Author Manuscript Author Manuscript

(E) Quantification of Nissl stain mean intensity in CA1 and dentate gyrus (DG) regions of the hippocampus, n = 3 Ogt-cKO and 4 control mice. See also Figure S2.
(F) Representative field of Golgi stain from CA1 pyramidal neurons and DG granule cell neurons in young Ogt-cKO and control mice.
(G) Quantification of spine number from tertiary dendrites of CA1 pyramidal neurons and DG granule cell neurons in Ogt-cKO and control mice; n = 10 neurons per mouse and 5 mice per group. Data are represented as mean ± SEM. *$p < 0.05$; **$p < 0.01$; t test (C–E and G).

Author Manuscript
Author Manuscript
Author Manuscript
Author Manuscript

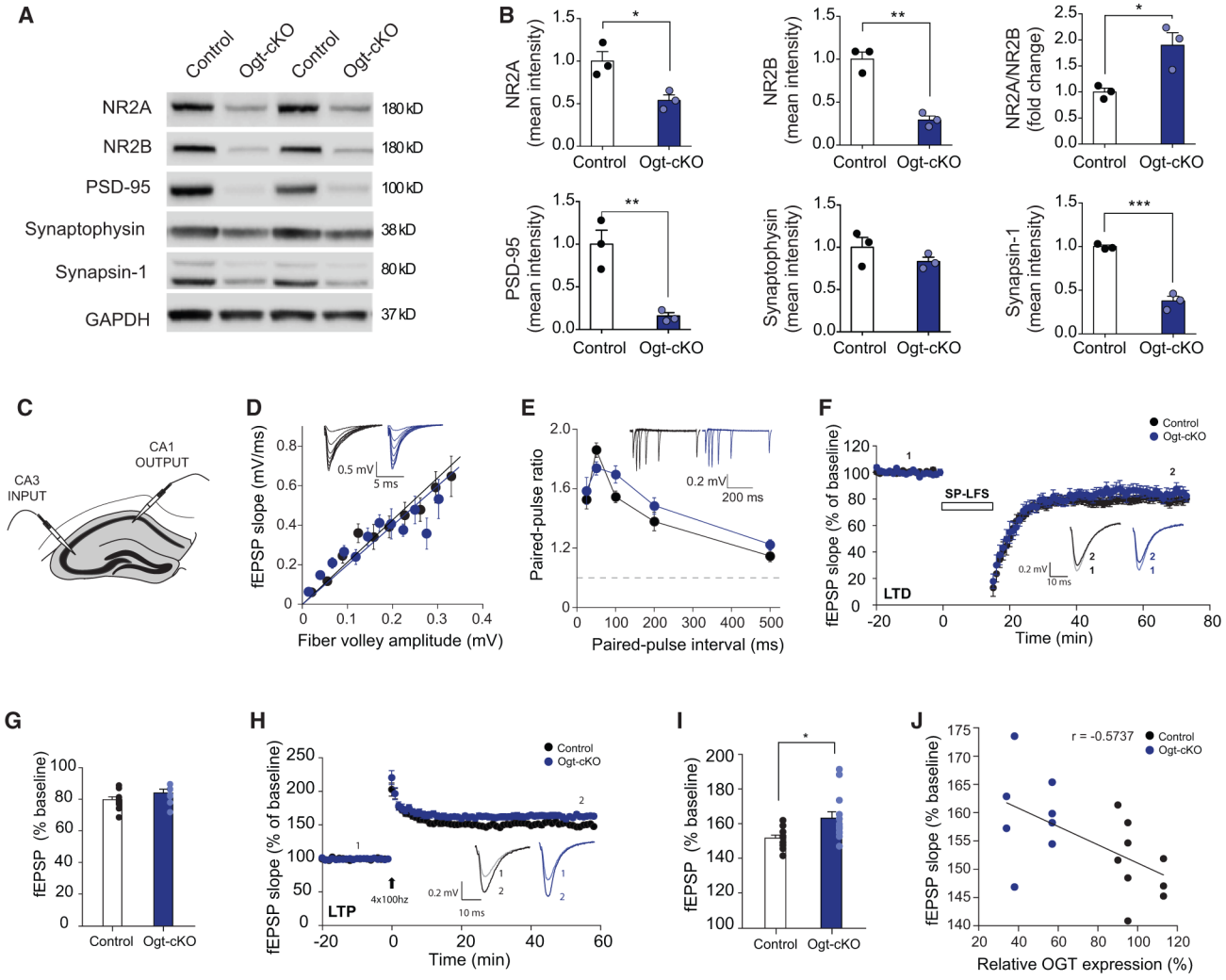

Figure 3. Abrogation of OGT in the Adult Brain Alters Hippocampal Synaptic Protein Expression and Function

(A) Representative western blot of synaptic proteins NR2A, NR2B PSD-95, Synaptophysin, and Synapsin-1 from whole hippocampal lysates of conditional excitatory neuron Ogt knockout (Ogt-cKO) and control mice.

(B) Quantification of synaptic protein expression from whole hippocampal lysates represented as mean optical intensity normalized to GAPDH. n = 3 mice per group.

(C) Schematic for electrophysiological recordings in CA3-CA1 neuronal projections, performed in *ex vivo* hippocampal slices from young adult Ogt-cKO or control mice.

(D) Basal transmission of CA3-CA1 measured as the Input-output relationship between presynaptic fiber volley amplitude and the slope of the resulting fEPSP. in acute hippocampal slices from 8- to 10-week-old control and Ogt-cKO mice, n = 10 slices/7 animals, n = 7 slices/3 animals, respectively.

(E) Paired-pulse facilitation measured at various timing delays.

(F) LTD recordings in the CA1 region of the hippocampus. The fEPSP slope is plotted as percentage of baseline average. Recordings were performed in acute hippocampal slices

Author Manuscript Author Manuscript Author Manuscript Author Manuscript

from 8- to 10-week-old control and Ogt-cKO mice, n = 10 slices/7 animals, n = 7 slices/3 animals, respectively) induced via 15 min single-pulse low-frequency stimulation (SP-LFS) (1 Hz).

(G) Bar graphs summarizing the average fEPSP slopes as a percentage of baseline, measured in the last 5 min of recording.

(H) LTP recordings in the CA1 region of the hippocampus of Ogt-cKO and control mice. The fEPSP slope is plotted as percentage of baseline average. Electrophysiological recordings were performed in acute slices from 8- to 10-week-old control and OGT-cKO mice n = 10 slices/6 animals, n = 13 slices/7 animals, respectively; LTP was induced via 4 trains of 100 Hz stimulation.

(I) Bar graphs summarizing the average fEPSP slopes as a percentage of baseline, measured in the last 5 min of recording.

(J) LTP magnitude shows a moderate correlation with levels of Ogt protein. Ogt levels were measured via western blot and plotted against average magnitude of LTP during last 5 min of recording.

Data are represented as mean ± SEM; *$p < 0.05$; **$p < 0.01$; ****$p < 0.0001$; t test (B, G, and I).

Author Manuscript Author Manuscript Author Manuscript Author Manuscript

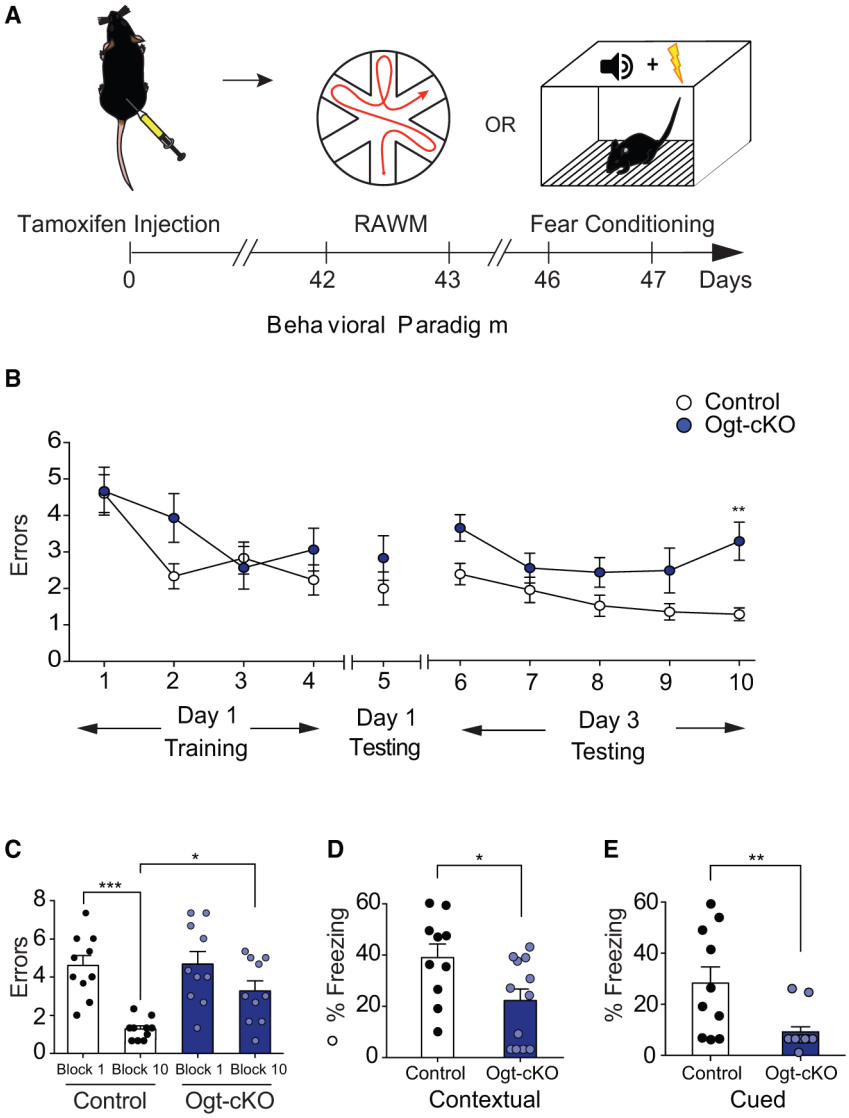

Figure 4. Abrogation of OGT in the Adult Brain Impairs Hippocampal-Dependent Learning and Memory

(A) Schematic depicting timeline for cognitive testing using radial arm water maze (RAWM) and fear conditioning behavioral paradigms in conditional Ogt knockout (Ogt-cKO) or control mice. See also Figure S3.

(B and C) Hippocampal-dependent spatial learning and memory was assessed in Ogt-cKO and control mice using RAWM. Quantification of the number of entry errors during RAWM training (B) and testing (B and C), n = 10 mice per group. See also Data S1. (D and E) Associative fear memory was assessed in Ogt-cKO and control mice using contextual (D) and cued (E) fear conditioning. Quantification of percentage of freezing 24 h after training; n = 12 Ogt-cKO and 10 control mice. See also Figure S3.

Data are represented as mean ± SEM; *p < 0.05; ***p < 0.001; repeated-measures ANOVA, Bonferroni post hoc test (B); one-way ANOVA, Tukey's post hoc test (C); t test (D and E).

Author Manuscript Author Manuscript Author Manuscript Author Manuscript

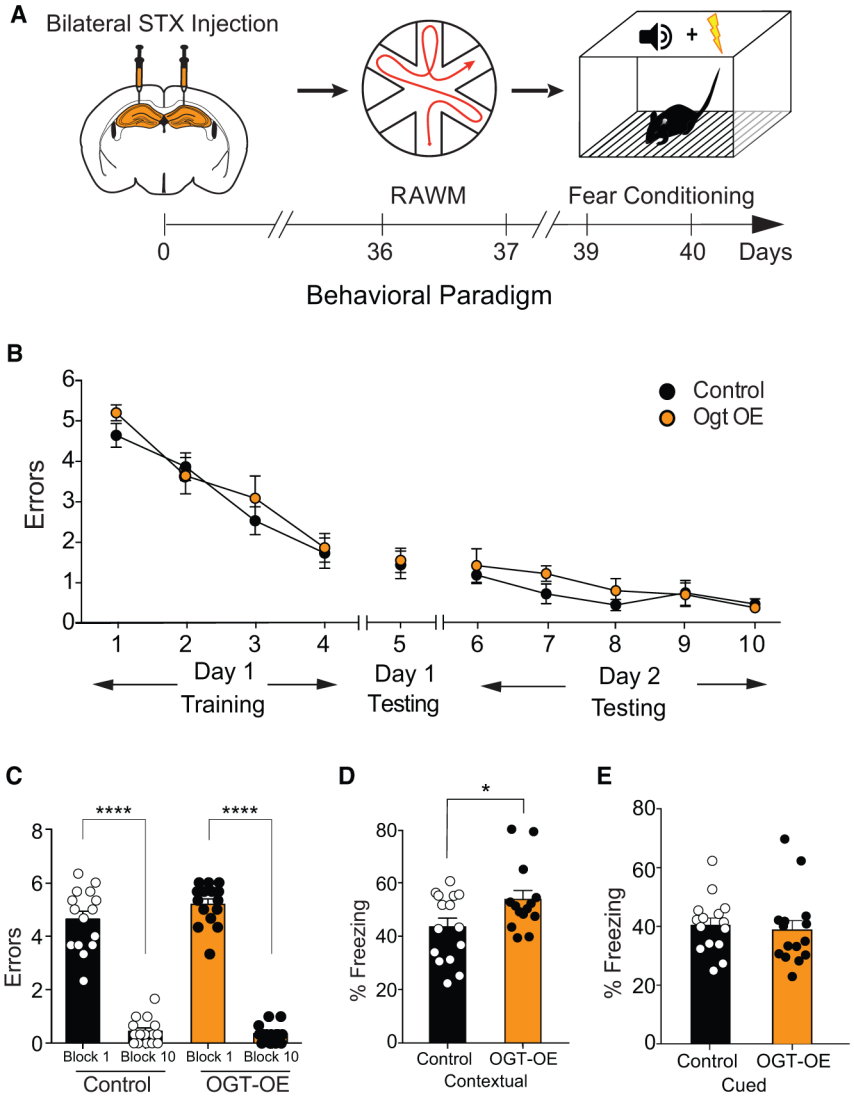

Figure 5. Increasing Neuronal OGT in the Young Adult Hippocampus Enhances Learning and Memory

(A) Schematic depicting experimental paradigm and timeline for cognitive testing using radial arm water maze (RAWM) and fear conditioning behavioral paradigms. Young adult (3 months) wild-type mice were given bilateral stereotaxic injections of lentivirus (LV) encoding either OGT (OGT-OE) or green florescent protein (GFP) control sequences driven by the neuron-specific Synapsin promoter into the hippocampus. See also Figures S4 and S5.

(B and C) Hippocampal-dependent spatial learning and memory was assessed in OGT-OE and GFP control-injected mice using RAWM. Quantification of the number of entry errors during RAWM training and testing (B) and long-term learning and memory testing (C); n = 15 mice for OGT-OE and control conditions. See also Data S1.

(D and E) Associative fear memory was assessed in Ogt-OE and GFP control-injected mice using contextual (D) and cued (E) fear conditioning. Quantification of percentage of

freezing 24 h after training, n = 15 mice for Ogt-OE and control conditions. See also Figure S5.

Data are represented as mean ± SEM; *p < 0.05; **p < 0.01; ****p < 0.0001; repeated-measures ANOVA, Bonferroni post hoc test (B); one-way ANOVA, Tukey's post hoc test (C); t test (D and E).

Author Manuscript Author Manuscript Author Manuscript Author Manuscript

Author Manuscript Author Manuscript Author Manuscript Author Manuscript

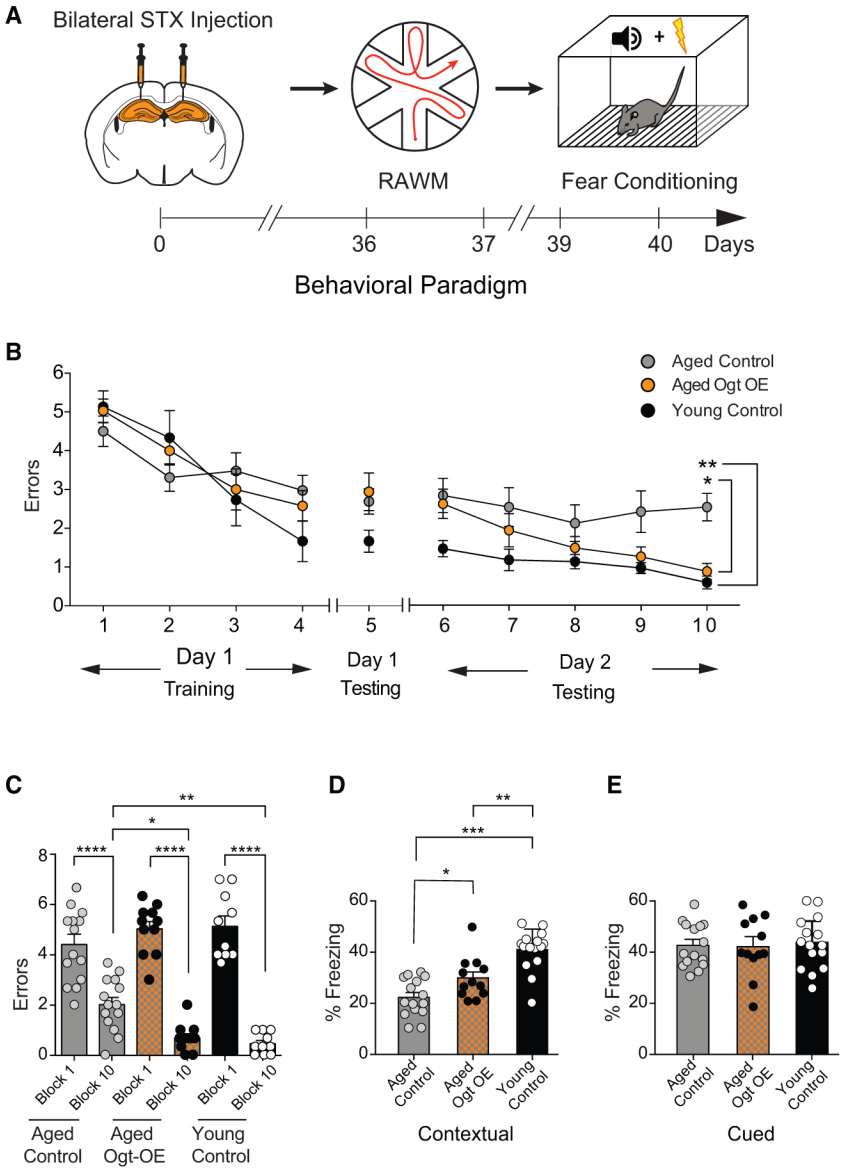

Figure 6. Increasing Neuronal OGT in the Aged Hippocampus Rescues Age-Related Cognitive Impairments

(A) Schematic depicting experimental paradigm and timeline for cognitive testing using radial arm water maze (RAWM) and fear-conditioning behavioral paradigms. Aged (21 months) wild-type mice were given bilateral stereotaxic injections of lentivirus (LV) encoding either OGT (OGT-OE) or green florescent protein (GFP) control sequences driven by the neuron-specific Synapsin promoter into the hippocampus. See also Figures S4 and S6.

(B and C) Hippocampal-dependent spatial learning and memory was assessed in OGT-OE and GFP control-injected aged mice and naive young adult (3 months) control mice using RAWM. Quantification of the number of entry errors during RAWM training and testing (B) and long-term learning and memory testing (C); n = 11 aged OGT-OE, 14 aged control, and 10 young control mice. See also Data S1.

Author Manuscript Author Manuscript Author Manuscript Author Manuscript

(D and E) Associative fear memory was assessed in OGT-OE and GFP control-injected aged mice and naive young adult control mice using contextual (D) and cued (E) fear conditioning. Quantification of percentage of freezing 24 h after training, n = 12 aged OGT-OE, 15 aged control, and 15 young control mice. See also Figure S6.

Data are represented as mean ± SEM; *p < 0.05; **p < 0. 01; ****p < 0.0001; repeated-measures ANOVA, Bonferroni's post hoc test (B); one-way ANOVA, Tukey's post hoc test (C–E).

Author Manuscript Author Manuscript Author Manuscript Author Manuscript

KEY RESOURCES TABLE

REAGENT or RESOURCE	SOURCE	IDENTIFIER
Antibodies		
Mouse anti-O-GlcNAc (RL2)	Abcam	ab2739; RRID: AB_303264
Rabbit anti-OGT (H-300)	Santa Cruz Biotech	sc-32921; RRID: AB_2156938
Rabbit anti-PSD-95	CS Technology	#2507; RRID: AB_561221
Rabbit anti-NR2B	Abcam	ab65783; RRID: AB_1658870
Rabbit anti-Synapsin-1	Abcam	ab18814; RRID: AB_444679
Mouse anti-Synaptoshysin (SY38)	EMD Millipore	MAB5258; RRID: AB_2313839
Mouse anti-GAPDH (6C5)	Abcam	ab8245; RRID: AB_2107448
Rabbit anti-Cleaved Caspase-3 (Asp175)	CS Technology	#9661; RRID: AB_2341188
Rabbit anti-c-Fos (Ab-5)	Calbiochem	#4-17; RRID: AB_2106755
Bacterial and Virus Strains		
LV-Syn-Ogt	This paper	N/A
LV-Syn-eGFP	This paper	N/A
Chemicals, Peptides, and Recombinant Proteins		
Tamoxifen	Sigma-Aldrich	T5648
Cresyl Violet	Sigma-Aldrich	C5042
Isoflurane (Isothesia)	Henry Schein	050033
10x RIPA Buffer	Abcam	AB156034
Protease inhibitor	Sigma-Aldrich	4693116001
PUGNAC	Sigma-Aldrich	A7229
Ketamine	Henry Schein	048858
Paraformaldehyde	Electron Microscopy Sciences	19210
Diaminobenzidine	Sigma-Aldrich	D5905
Entellan	Thermo Fisher Scientific	14800
Citrisolv	Thermo Fisher Scientific	22143975
TRIZol	Thermo Fisher Scientific	15596026
Critical Commercial Assays		
FD Rapid Golgi Stain Kit	Thermo Fisher Scientific	NC0292960
Clarity ECL	Bio-Rad	1705060
ABC Kit	Vector Laboratories	PK-6100
PureLink RNA Mini Kit	Thermo Fisher Scientific	12183020
High Capacity cDNA Reverse Transcription Kit	Thermo Fisher Scientific	4368813
Experimental Models: Organisms/Strains		
C57BL/6J	Jackson Laboratory	#000664
Ogt$^{flox/y}$	Jackson Laboratory	#004860
CamK2a-CreER^{T2}	Jackson Laboratory	#012362
Oligonucleotides		
Primer Ogt floxed forward: CAT CTC TCC AGC CCC ACA AAC TG	This paper	N/A

Author Manuscript Author Manuscript Author Manuscript Author Manuscript

REAGENT or RESOURCE	SOURCE	IDENTIFIER
Primer Ogt floxed reverse: GAC GAA GCA GGA GGG GAG AGC AC	This paper	N/A
Primer Cre forward: AGC TCG TCA ATC AAG CTG GT	This paper	N/A
Primer Cre reverse: CAG GTT CTT GCG AAC CTC AT	This paper	N/A
Primer Myogenin forward: TTA CGT CCA TCG TGG ACA GC	This paper	N/A
Primer Myogenin reverse: TGG GCT GGG TGT TAG CCT TA	This paper	N/A
Primer Ogt forward: CAC CGT TCA GTA TTC TGT GCC GCC	This paper	N/A
Primer Ogt reverse: TAG GGC AAT TCT CCT GTG CG	This paper	N/A
Recombinant DNA		
LV-Syn-Ogt	This paper	N/A
LV-Syn-GFP	This paper	N/A
pENTR D-TOPO	Thermo Fisher Scientific	K240020
Software and Algorithms		
GraphPad Prism 5.0	GraphPad	https://www.graphpad.com/scientific-software/prism/
FreezeScan	Cever Sys	http://cleversysinc.com/CleverSysInc/
MotorMonitor	Kinder Scientific	http://kinderscientific.com/products/open_field/
FIJI ImageJ 1.x	NIH	PMID 22930834